Talanta 296 (2026) 128438

Contents lists available at ScienceDirect

Talanta

journal homepage: www.elsevier.com/locate/talanta

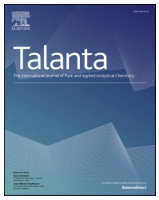

Electrochemical immunosensing for rapid glaucoma disease diagnosis through simultaneous determination of SPP1 and GAS6 proteins in ocular fluids

Eloy Povedano [a], Raquel Rejas-González [b], Ana Montero-Calle [b], Beatriz Arévalo [a], Alejandro Valverde [a], Natalia Pastora Salvador [c], María José Crespo Carballés [c], Juan Sánchez-Naves [d], José M. Pingarrón [a], Rodrigo Barderas [b,e,*], Susana Campuzano [a,e,**], Ana Guzman-Aranguez [f,***]

[a] Department of Analytical Chemistry, Faculty of Chemical Sciences, Complutense University of Madrid, Plaza de las Ciencias 2, 28040, Madrid, Spain
[b] Chronic Disease Programme, UFIEC, Institute of Health Carlos III, Majadahonda, 28220, Madrid, Spain
[c] Opthalmology Service, Hospital Universitario Infanta Leonor, 28031, Madrid, Spain
[d] Oftalmedic Salvà, 07013, Palma, Illes Balears, Spain
[e] CIBER of Frailty and Healthy Aging (CIBERFES), Instituto de Salud Carlos III, 28046, Madrid, Spain
[f] Biochemistry and Molecular Biology Department, Faculty of Optics and Optometry, Complutense University of Madrid, 28037, Madrid, Spain

ARTICLE INFO

Keywords:
Osteopontin (SPP1)
Growth arrest-specific 6 (GAS6)
Electrochemical bio-sensing technology
Timely diagnosis
Glaucoma
Aqueous humor

ABSTRACT

The present work reports the development of the first electrochemical immunoplatform for the simultaneous determination of Osteopontin (SPP1) and Growth Arrest-Specific 6 (GAS6) proteins, novel glaucoma-related biomarkers, involving magnetic microparticles (μMPs), specific capture (CAb) and detection (DAb) antibodies further labeled with horseradish peroxidase (HRP) for the selective and sensitive sandwiching of both proteins and amperometric detection at disposable screen-printed carbon electrodes (SPCEs). The dual immunoplatform exhibited very attractive sensitivity, reproducibility and selectivity for the determination of both biotargets at the required clinical levels (LOD values of 6.0 and 59.0 pg mL^{-1} for SPP1 and GAS6, respectively). The analysis can be simply performed in less than 90 min. The dual immunoplatform was applied with very promising results to the analysis of aqueous humor samples from Implantable Collamer Lens (ICL), cataracts (CAT), and glaucoma (GLAU) patients. The diagnostic usefulness of SPP1 and GAS6 determination to discriminate between the three types of patients and its potential as a simple, rapid, and minimally invasive tool to support early diagnosis and follow-up of GLAU disease was proved. In addition, a proof-of-concept test using tear samples from a healthy volunteer supports the possibility of detecting these markers in this type of sample.

1. Introduction

Glaucoma is a disease that injures the optic nerve and is characterized by the gradual death of retinal ganglion cells and their axons, resulting in a continuous and progressive loss of vision [1,2]. It is the leading cause of irreversible blindness worldwide, affecting more than 70 million people. Furthermore, considering the greater longevity and aging of the population, it is estimated that its prevalence will increase to more than 110 million by 2040, generating a high impact on both social dependence among the elderly and economic on health systems [1–3].

Among the different types of glaucoma, the most common, also known as silent blindness, is the primary open-angle glaucoma. Although it is an irreversible pathology, its early diagnosis assists in the

* Corresponding author. Chronic Disease Programme, UFIEC, Institute of Health Carlos III, Majadahonda, 28220, Madrid, Spain.
** Corresponding author. Department of Analytical Chemistry, Faculty of Chemical Sciences, Complutense University of Madrid, Plaza de las Ciencias 2, 28040 Madrid, Spain.
*** Corresponding author. Biochemistry and Molecular Biology Department, Faculty of Optics and Optometry, Complutense University of Madrid, 28037, Madrid, Spain.
E-mail addresses: r.barderasm@isciii.es (R. Barderas), susanacr@quim.ucm.es (S. Campuzano), aguzman@opt.ucm.es (A. Guzman-Aranguez).

https://doi.org/10.1016/j.talanta.2025.128438
Received 12 April 2025; Received in revised form 22 May 2025; Accepted 5 June 2025
Available online 6 June 2025

timely administration of treatments that contribute to slowing its progression. However, due to its asymptomatic nature in early stages, the disease frequently remains undetected until it has progressed significantly. Consequently, the diagnosis is often delayed, limiting opportunities for timely intervention [3,4]. Unfortunately, more than 50 and 90 % of glaucoma patients are undiagnosed in high and lower-middle income countries, respectively [4].

Although the underlying causes of glaucoma remain uncertain, elevated intraocular pressure (IOP) is a common feature in most forms of the disease. Currently, glaucoma diagnosis relies on eye examinations, including pupil dilation and IOP measurement. However, elevated IOP is often detected only after significant visual field loss delaying diagnosis. Current therapeutic actions are focused on reducing IOP through pharmacological or laser interventions, with surgical options pursued if these methods prove ineffective to drain the fluid from the eye [2,5]. However, the recurrence of vision loss in patients despite successful IOP control underscores that IOP is not the sole determinant in disease progression and that its management alone is insufficient to halt or delay disease advancement [2,6].

Therefore, the identification of novel glaucoma-related biomarkers, or *"glaukers"*, with the potential and ability to assist in non-invasive early diagnosis and to elucidate the pathological mechanisms and underlying causes of glaucoma, represents a critical and challenging high-priority research area [2,7,8]. These "*glaukers*" might serve as therapeutic targets to improve the diagnosis, monitoring of disease progression, or assessment of response to treatment.

Aqueous humor and tears are essential ocular fluids that maintain eye homeostasis by providing nutrients and removing waste. These ocular fluids are among the most valuable sources of biomarkers for eye diseases due to their direct contact with the eye's physiological and pathological environment, thus offering a more targeted and enriched source of disease-related biomarkers. Additionally, their collection is non-invasive (tears) or minimally invasive (aqueous humors during cataracts intervention) compared to tissue biopsies, making them highly suitable for early disease detection. Advances in proteomics and metabolomics have further enhanced the potential of these fluids in identifying novel diagnostic and prognostic markers [2,9].

In this context, the proteins SPP1 (Osteopontin) and GAS6 (Growth arrest-specific 6) have been identified as potential biomarkers in glaucoma and cataracts [2]. SPP1 is involved in neuroinflammation and tissue remodeling [10,11], while GAS6 plays a role in cell survival and apoptosis modulation [12]. Given their relevance in the pathophysiology of the disease, the early detection of GAS6 and SPP1 may facilitate the potential diagnosis of glaucoma.

Moreover, electroanalytical technologies, and particularly those combining immunosensing strategies implemented on the surface of magnetic microparticles (μMPs) coupled to disposable electrode substrates for single or multiplexed amperometric transduction, emerge as an ideal alternative to allow a simpler and more affordable determination in any environment compared to the ELISA methodologies available for their analysis in plasma and serum samples. Considering this state of the art, this work takes advantage of a technology that we proposed for the determination of GAS6 [13] to develop a method for the quantification of SPP1 and performing the integration of both methods in a pioneering platform for their simultaneous determination. After the corresponding characterization, the dual immunoplatform is applied to the analysis of aqueous humor from ICL, CAT, and GLAU patients and as a proof of concept in raw tear samples, biological matrices not previously explored with electroanalytical technologies. There is a wide acceptance that simultaneous determination of multiple biomolecules in a single assay maximizes the information obtained from limited reagents and sample volumes and improves efficiency and speeds up the diagnostic process [14,15]. Therefore, several electrochemical immunotechnologies for dual determinations [16], some of them also leveraging the advantages of using μMPs [17], are available in the literature. Nevertheless, this work can be considered as innovative in both the biotargets interrogated and the scenario in which they are determined (GLAU screening). So far, only electrochemical biosensors for the single determination of SPP1 [18,19] and GAS6 [13] have been reported, but none for the simultaneous determination of SPP1 and GAS6. Moreover, only the GAS6 biosensor was applied to the analysis of real samples.

2. Materials and methods

2.1. Equipment and electrodes

Amperometric measurements were conducted at room temperature, using a multiple potentiostat-galvanostat μStat 8000 (Metrohm-DropSens) controlled by DropView 8400 and a potentiostat (model 812B, CH Instruments, Austin, TX) controlled by CHI812B software, for the single and dual readings, respectively. Individual and dual screen-printed carbon electrodes composed of, respectively, one circular (SPCE, DRP-110, $\phi = 4$ mm, A = 12.57 mm^2) or two elliptical (SP_dCE, DRP-1110, $\phi_1 = 4$ mm, $\phi_2 = 1.7$ mm, A = 4.71 mm^2), working electrodes (WE), used as electrochemical transducers, and their corresponding specific SPCE (DRP-CAC) and SP_dCE (DRP-BICAC) connection cables, were purchased from Metrohm-DropSens. A custom-made polymethylmethacrylate (PMMA) enclosure with one or two inlaid neodymium magnets (AIMAN GZ) were used for the efficient and reproducible capture of the magnetic bioconjugates on the WE/s surface/s of the SPCE or SP_dCE, respectively.

Other apparatus used were: a magnetic separator (Dynamag™-2, Cat. No. 12321D, Invitrogen™) for the manipulation of the μMPs, an incubator shaker (Optic Ivymen® System, Comecta S.A, Sharlab) for the μMPs modification processes, a vortex mixer (F202A0173, Velp Scientifica) for the homogenization of the solutions, a MicroMagmix magnetic stirrer (MCG05E, OVAN), and a precision Crison Basic 20^+ pH-meter (Orion Star A214 model, Thermo-Scientific).

2.2. Reagents and solutions

All the reagents used were of the highest available analytical grade. μMPs modified with carboxylic acid groups (COOH-μMPs, $\phi = 2.7$ μm, 10 mg mL^{-1}, Dynabeads M − 270 Carboxylic acid, Cat. No. 14305D) were purchased from Invitrogen-ThermoFisher™. Recombinant human Osteopontin standard (SPP1), mouse anti-human Osteopontin capture antibody (SPP1-CAb), and biotinylated goat anti-human Osteopontin detection antibody (SPP1-bDAb) were components of the Human Osteopontin kit (Cat. No. DY1433), and recombinant human Growth Arrest-Specific Protein 6 (GAS6) standard, goat anti-human GAS6 capture antibody (GAS6-CAb), and biotinylated goat anti-human GAS6 detection antibody (GAS6-bDAb) were components of the Human GAS6 kit (Cat. No. DY885B). Both kits were purchased from R&D Systems.

All capture and detection antibodies, as well as the synthetic standards used in this work, were reconstituted after receipt in the corresponding sterilized buffer solution and stored in small aliquots at −40 or −80 °C until use, according to the manufacturer's specifications.

Other reagents used in this research include: NaCl, KCl, NaH_2PO_4, Na_2HPO_4, and Tris-HCl from Scharlab; N-(3-dimethylaminopropyl)-N′-ethylcarbodiimide (EDC), and N-hydroxysulfosuccinimide (NHSS) from Fluorochem; ethanolamine (ET), hydroquinone (HQ), and hydrogen peroxide (H_2O_2, 30 % w/v) from Sigma-Aldrich; and 2-(N-morpholino) ethanesulfonic acid (MES) from Gerbu. A high sensitivity streptavidin-horseradish peroxidase conjugate (Strep-HRP) and a blocker casein solution (a 1 % w/v purified casein ready-to-use PBS solution, BB) were procured by Roche and Thermo Fisher Scientific, respectively.

All buffer solutions were prepared in Milli-Q water (18 MΩ cm at 25 °C): PBS consisting of 10 mM phosphate buffer solution (PB) containing 137 mM NaCl and 2.7 mM KCl (pH 7.5); Tris-HCl (10 mM, pH 7.2); MES (25 mM, pH 5); PB (50 mM, pH 6); and PB (100 mM, pH 8).

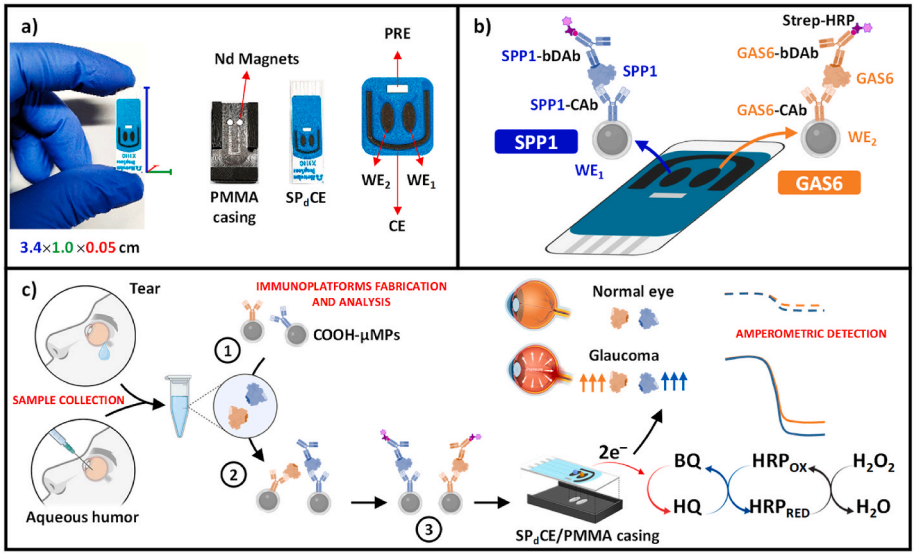

Fig. 1. a) Images of the SP_dCE dual electrochemical transducers and PMMA housing used to obtain amperometric readings. b) Schematic of the dual SPP1/GAS6 immunoplatform based on sandwich immunoassay formats and enzymatic labeling with the HRP enzyme. c) Immunoreaction and amperometric transduction processes involved in the dual determination of SPP1/GAS6 proteins, and fictitious amperometric responses obtained in the analysis of SPP1 and GAS6 proteins in tear/aqueous humor samples collected from normal and glaucoma eyes. Created in part with biorender.com.

2.3. Immunoconjugates assembly on μMPs

The biofunctionalization of COOH-μMPs was accomplished in 1.5 mL microcentrifuge tubes by sequential implementation of incubation (25 μL, using an incubator shaker at 25 °C and 950 rpm) and washing (50 μL) steps using the appropriate bioreagent or buffer solution, respectively. In both cases, the supernatant was removed by magnetizing the μMPs suspension for 3 min using a magnetic concentrator. Briefly, for each determination, a 3.0 μL aliquot of the commercial COOH-μMPs suspension was placed in a 1.5 mL microcentrifuge tube and washed twice with MES buffer (10 min at 25 °C and 950 rpm). Next, to biofunctionalize the COOH-μMPs, an initial activation step was made to derivatize carboxylic groups into a semi-stable amine-reactive ester group through their incubation with an EDC/NHSS solution for 35 min. After two washings with MES buffer, the covalent attachment of the biorecognition element was performed by incubating the activated COOH-μMPs with the SPP1-CAb (25 μg mL^{-1}) or GAS6-CAb (2.5 μg mL^{-1}) solution (both prepared in MES buffer) for 60 or 15 min, respectively. Then, after two additional washes with MES buffer, a blocking step of the remaining active groups to prevent possible non-specific adsorptions of other bioreagents or biomolecules coexisting in the sample, was conducted by incubating the CAb-μMPs with an ET solution (1 M, prepared in PB 100 mM, pH 8) for 60 min. Thereafter, one washing with Tris-HCl followed by another two with PBS solution were performed. The blocked CAb-μMPs were stored at 4 °C in filtered PBS until use.

Starting from the blocked CAb-μMPs, two different optimized protocols were followed for the determination of SPP1 or GAS6.

The blocked SPP1-CAb-μMPs were incubated with a mixture solution containing the bDAb (0.5 μg mL^{-1}) and the SPP1 standard or analyzed sample (prepared in PBS) for 30 min, followed by another incubation step in a Strep-HRP solution (2500 times diluted in BB) for 30 min.

The blocked GAS6-CAb-μMPs were sequentially incubated in three different independent solutions: i) GAS6 standard or tested sample (prepared in PBS), ii) bDAb (2.5 μg mL^{-1}, prepared in BB), and iii) Strep-HRP (1000 times diluted in BB) for 45, 15 and 15 min, respectively.

In both protocols, two washings with BB were performed between and after the incubation steps. Finally, the resulting biofunctionalized μMPs were re-suspended in 50 or 10 μL of PB (50 mM, pH 6) for the amperometric measurements at SPCEs or SP_dCEs, respectively.

2.4. Amperometric measurements

To perform each single or dual amperometric reading, 50 or 10 μL of the modified μMPs suspension were reproducibly trapped on the WE surface(s) of a new SPCE or SP_dCE previously assembled in their appropriate PMMA housing.

The PMMA-housing/$SP_{(d)}CE$-μMPs setup was connected to the potentiostat with the specific cable and immersed into an electrochemical cell containing 10 mL of a freshly prepared PB solution (50 mM, pH 6.0) with 1.0 mM HQ. While maintaining continuous mechanical stirring, a constant potential difference of −0.20 V relative to the Ag pseudo-reference electrode was applied. When the background current was stabilized, 50 μL of a 0.1 M H_2O_2 solution was added to the cell and the variation in the cathodic current was monitored until a steady state was reached, typically within 100 s. The parameters influencing the amperometric detection, such as the applied potential, the composition and pH of the supporting electrolyte, the concentrations of the enzyme substrate (H_2O_2), and the electrochemical mediator (HQ), as well as the experimental protocol to ensure consistent magnetic capture of the μMPs on the WE surface of $SP_{(d)}CEs$, were optimized in previous works [20,21]. Regarding the pH at which the detection was carried out, it is important to mention that we previously studied the influence of the measurement medium pH on the performance of a direct competitive immunosensor using amperometric transduction with the HRP/H_2O_2/HQ system. We found that the best amperometric signals were obtained working in phosphate buffer solution at pH 6.0 [20], demonstrating the stability of the immune complexes at this pH value. These results also agreed with those provided by other studies reporting an optimal activity of HRP at pH 6.0 [22,23].

The amperometric signals represent the difference between the steady state and the background currents which were measured, respectively, after and before the addition of H_2O_2 to the electrochemical cell. Mean values of three independent replicates, with error bars indicating the standard deviation (SD) of these replicates were used. Confidence intervals were calculated at a significance level of $\alpha = 0.05$.

2.5. Analysis of aqueous humor and tear samples

The developed methods were applied to the determination of the

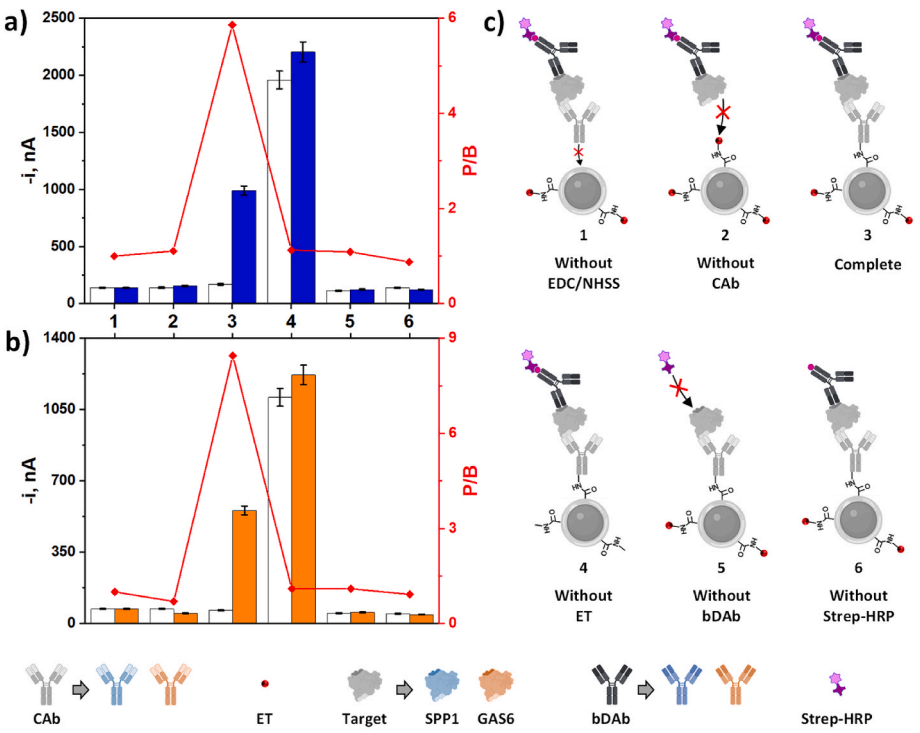

Fig. 2. Feasibility of the developed immunosensing strategies for the single determination of SPP1 (a) and GAS6 (b) proteins. Comparison of the amperometric responses obtained for 0 (white bars, B signals) and 500/1000 (blue/orange bars, P signals) pg mL^{-1} of SPP1/GAS6, as well as the resulting P/B ratio (red points and lines). Different immunoplatforms were constructed from unmodified μMPs (without immobilized CAb, omitting the incubation of: EDC/NHSS during the activation step (1) or CAb (2)) and CAb-μMPs (without ET incubation in the blocking step (4), in the absence (5) and in the presence (3, 6) of bDAb, and in the absence of Strep-HRP (6)). c) Schematic representations of each tested control experiment. Created in part with biorender.com.

target proteins in aqueous humor samples from Implantable Collamer Lens (ICL), cataracts (CAT), and glaucoma (GLAU) patients (5 of each, see Table S1 in the Supporting Information) and as a proof of concept also in tear samples from a healthy volunteer.

The clinical and ethical aspects of this study were reviewed and approved by the Clinical Research Ethics Committee of Hospital Universitario Infanta Leonor (Madrid, Spain) (CEIC 011–23) and the Ophthalmedic and I.P.O. Institute (Palma de Mallorca, Spain). Written informed consent was obtained from all participants, allowing the use of their biological samples for research purposes. The study complied with ethical guidelines established by Spanish legislation (LOPD 15/1999) and the European Union's Charter of Fundamental Rights (2000/C364/01). Patient data were handled in accordance with the Declaration of Helsinki (latest revision, 2013) and Spain's National Biomedical Research Law (14/2007, of July 3rd).

Aqueous humor samples were collected at the onset of surgery following the administration of 2 % (w/v) lidocaine anesthetic drops. A 30-gauge Rycroft cannula, connected to a 1 mL tuberculin syringe, was used for extraction as previously described [24]. Per patient, 0.05–0.15 mL of aqueous humor was obtained and immediately stored at −20 °C, with subsequent preservation at −80 °C.

2.6. Statistical analysis

Non-parametric Mann-Whitney *U* test values (p-values) were calculated using R (v3.6.2); p-values ≤0.05 were considered statistically significant. ROC curves (Receiver Operating Characteristic Curve) of SPP1 and GAS6 individually or in combination, and correlations, were obtained with R (version 3.6.2), using the "ModelGood" and the "Epi" packages to determine the diagnostic ability of the test.

3. Results and discussion

This work reports the first electrochemical immunoplatform for the rapid, direct, and simultaneous amperometric determination of SPP1 and GAS6 proteins using a single 25 μL sample drop of raw tear or 50 to 100-fold diluted aqueous humor samples. As shown in Fig. 1, the dual SPP1/GAS6 immunoplatform was developed by functionalizing independent batches of μMPs with the specific immunoreagents for the selective capture and detection of each protein using sandwich immunoassay configurations. The resulting modified μMPs assemblies were integrated into a dual electrochemical transducer by simply trapping the μMPs droplets onto neighboring WEs through magnetic attraction. Finally, a short (~100 s) and simultaneous amperometric transduction step at −0.2 V (vs. Ag *pseudo*-reference electrode) was performed for the determination of both proteins, based on enzymatic labeling with the HRP enzyme using HQ/H_2O_2 as mediator/substrate redox system.

To ensure the optimal performance of the dual immunoplatform special attention was paid to tackling the key operational and detection-related challenges, including: (i) verifying the viability of both immunoassays while establishing the reliability of the amperometric signals obtained; (ii) achieving highly sensitive assays, involving the possible shortest analysis time and the simplest protocols, as well as using sample volumes in the μL-range; (iii) addressing potential interference or cross-talking during the immuno-recognition and amperometric transduction processes, respectively; and (iv) developing a robust μMPs modification protocol for the reliable and reproducible fabrication of the dual immunoplatform.

These challenges were addressed by optimizing the main parameters involved in the implementation of the immunoassays and the amperometric transduction.

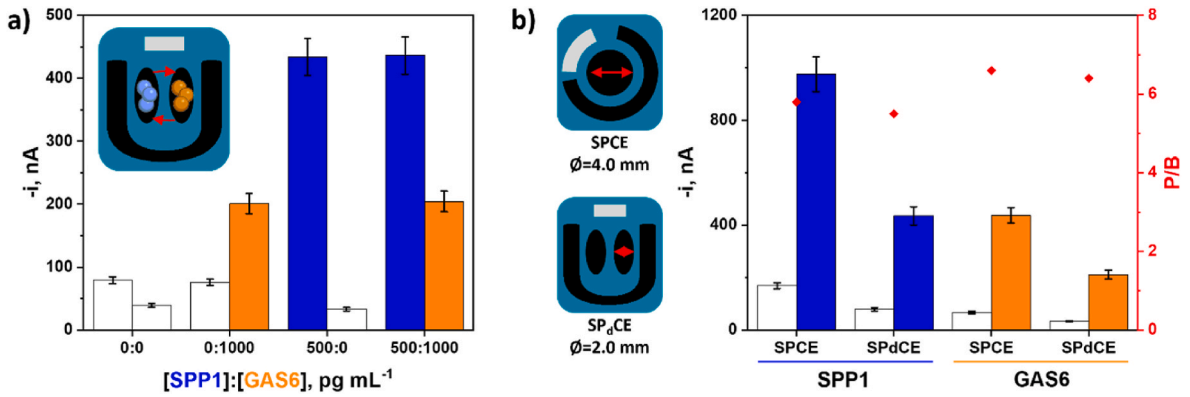

Fig. 3. Feasibility of the simultaneous detection of SPP1 and GAS6 by using dual immunoplatforms. Crosstalk assessment between neighboring WEs: amperometric responses obtained for mixtures prepared with different concentrations of the two proteins (a). Evaluation of the differences in the currents measured with single (SPCE) or dual (SP_dCE) electrodes. Amperometric responses in the absence (B, white bars) and in the presence (P, blue/orange bars) of 500/1000 pg mL^{-1} of SPP1/GAS6 proteins as well as the resulting P/B ratio values (red points) (b). Created in part with biorender.com.

3.1. *Feasibility and optimization of the individual immunoplatforms*

The feasibility of the proposed methodology for the construction of the immunosensors and the reliability of the amperometric responses they provide were verified by evaluating the performance of the two immunodetection strategies developed for the single determination of SPP1 and GAS6 proteins.

The amperometric responses obtained with each methodology were measured in the absence (0 pg mL^{-1}, white bars, B signals) and the presence (500/1000 pg mL^{-1}, blue/orange bars, P signals) of the corresponding target protein, SPP1/GAS6. These measurements were conducted using a key set of control experiments, designed by omitting the incubation of fundamental bioreagents required for the construction of the immunosensors. The results obtained, shown in Fig. 2, highlight the negative impact of omitting certain bioreagents on the performance of both immunodetection strategies. These results support the rational design and proper functioning of the proposed strategies and confirm the absence of non-specific adsorptions and the reliability of the amperometric measurements for the detection of both target proteins, exclusively attributed to the specific interactions between the required bioreagents (bars 3 in Fig. 2).

Considering that the experimental variables for the single determination of the GAS6 protein were reported in a previous work [13], the key variables for the determination of SPP1 were now evaluated and selected. Therefore, the amperometric measurements obtained for 0 (gray bars, B) and 500 (blue bars, P) pg mL^{-1} of SPP1 and the resulting P/B ratio were compared, taking the largest value of this ratio as a selection criterion.

All the tested variables, their ranges and the values selected for each target determination, are displayed in Fig. S1 and summarized in Table S2 (both in Supporting Information). Optimized variables included the concentration and incubation time of CAb, the protocol followed for sandwich immunoassay preparation (1–3 incubation steps, see details in Table S2), and the concentration and incubation time of bDAb and Strep-HRP.

Other experimental variables such as COOH-μMPs suspension volume, EDC/NHSS, and ET concentrations, as well as the incubation times during the COOH-μMPs surface activation and blocking steps for CAb-μMPs preparation, were kept consistent with the reported values for other sandwich immunoplatforms we developed [13,25].

3.2. *Crosstalk evaluation, feasibility, and implementation of the dual SPP1/GAS6 immunoplatform*

The immunoplatforms developed for the single determination of SPP1 and GAS6 proteins were integrated into a disposable dual

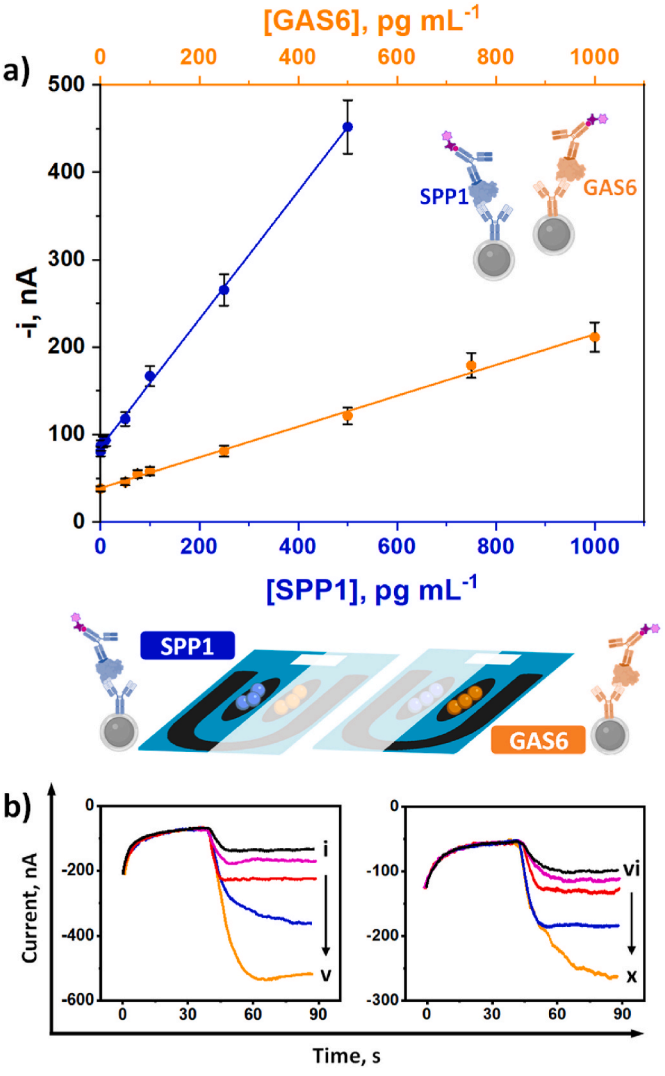

Fig. 4. Performance of the SPP1/GAS6 dual immunoplatform. Calibration plots (a) and real amperometric traces (b) recorded with the dual immunoplatform for the simultaneous determination of SPP1 and GAS6. Created in part with biorender.com.

Table 1
Analytical and operational characteristics obtained with SPCE and SP_dCE immunoplatforms for the single or dual determination of SPP1 and GAS6 proteins, respectively.

	SPP1 Immunoplatform		GAS6 Immunoplatform	
Parameter	SPCE	SP_dCE	SPCE	SP_dCE
Linear dependence	i_c *vs.* [SPP1]		i_c *vs.* [GAS6]	
Intercept, nA	153 ± 25	86 ± 5	101 ± 61	39 ± 6
Slope, nA mL pg^{-1}	1.65 ± 0.04	0.73 ± 0.02	0.44 ± 0.02	0.18 ± 0.01
LR, pg mL^{-1}	4.2–1500	20–500	62–5000	197–1000
LOD, pg mL^{-1}	1.3	6.0	19	59
LOQ, pg mL^{-1}	4.2	20	62	197
RSD$_{(Same\ day)}$, %	4.0$_{(n = 10);\ 500\ pg\ mL^{-1}}$	–	3.9$_{(n = 10);\ 5000\ pg\ mL^{-1}}$	–
RSD$_{(Different\ days)}$, %	8.5$_{(n = 10);\ 500\ pg\ mL^{-1}}$	6.8$_{(n = 5);\ 100\ pg\ mL^{-1}}$	8.2$_{(n = 10);\ 5000\ pg\ mL^{-1}}$	8.0$_{(n = 5);\ 500\ pg\ mL^{-1}}$
Stability, days	30 (No longer times were assayed)		3	

immunoplatform with 2 carbon WEs. This immunoplatform allowed the simultaneous determination of the two proteins by modifying each sensing surface with the μMPs bearing the corresponding sandwich immunocomplexes for each biomarker.

To ensure the reliable simultaneous determination of both proteins, it is essential to rule out any possible crosstalk between the two neighboring working electrodes during the transduction process. To check this, independent batches of μMPs were prepared and the amperometric responses obtained for each target protein on the corresponding immunosensor were compared for mixture solutions of the two proteins. As shown in Fig. 3a), the responses measured for SPP1 were not affected by the presence of GAS6 on the adjacent electrode, and viceversa, indicating that there was no apparent cross-talking, supporting the suitability of the dual immunoplatform for the simultaneous determination of these biomarkers.

Thereafter, the amperometric responses obtained in the absence and in the presence of 500/1000 pg mL^{-1} of SPP1/GAS6 proteins, using single SPCE or dual SP_dCE transducers were compared (Fig. 3b). As expected, the amperometric responses at SP_dCEs were smaller than those recorded with SPCEs, which is due to both the smaller active surface area and the higher diffusion barrier on the WE surface of the dual electrodes after trapping the same amount of μMPs on a 2.7 times smaller surface area (4.71 *vs.* 12.57 mm^2). However, despite the decrease in the measured responses, no significant differences were observed in the P/B ratios for each biomarker working with both transducers.

3.3. Analytical and operational performance of the dual SPP1/GAS6 immunoplatform

The analytical and operational performance of the developed dual immunoplatform was evaluated for the simultaneous determination of SPP1 and GAS6 "*glaukers*". The amperometric responses obtained for increasing concentrations of SPP1 and GAS6 protein standards in buffered solutions and the resulting calibration plots are shown in Fig. 4a) and b), respectively. Such plots exhibited a linear dependence between the cathodic current and the protein concentrations over the 20–500 and 197–1000 pg mL^{-1} ranges for SPP1 and GAS6, respectively. Table 1 compares the analytical and operational parameters obtained for both single and dual determination of SPP1 and GAS6 proteins using SPCEs and SP_dCEs, respectively. In agreement with results discussed in the previous section, the slopes of the calibration curves were reduced by a factor of 2.3 (SPP1) and 2.5 (GAS6) times when switching from SPCEs to SP_dCEs.

The estimated limits of detection (LOD) values (3 × s_b/m criterion; s_b: standard deviation of 10 B signals; m: slope of the calibration graph), were 6 (SPP1) and 59 (GAS6) pg mL^{-1}, demonstrating the suitability of the developed dual immunoplatform for the determination of both biomarkers at their physiological levels in aqueous humor [2].

It is important to highlight that, although there are electrochemical biosensors reported in the literature for the single determination of SPP1 with slightly lower claimed LODs, 5 pg mL^{-1} [18] or 0.3 pg mL^{-1} [19], they have not been applied in real samples. Regarding GAS6, only the electrochemical immunosensor developed by our group appears in the literature. This immunosensor was applied to the analysis of plasma samples from patients suffering heart failure and diagnosed with pancreatic ductal adenocarcinoma [13]. Moreover, the commercial ELISA kits that use the same immunoreagents employed in the dual immunoplatform claimed a similar detectability (≤62.5 pg mL^{-1} for SPP1 [26] and ≤15.6 pg mL^{-1} for GAS6 [27]). Nevertheless, the electrochemical immunoplatform provides significant advantages such a notably shorter assay time (60–75 min vs. 4 h 40 min starting from CAb coated μMPs and ELISA plates, respectively), compatibility with affordable instrumentation, applicability at the point of need, and dual determination.

Since each measurement implies the use of a new electrode and batch of magnetic immunoconjugates, it is crucial to ensure the robustness of the protocols used both in the immunoplatform preparation and the amperometric measurements. For this purpose, the amperometric responses provided involving 5 different SP_dCEs and immunoconjugates batches, which were prepared on the same day under the same conditions, were measured for 100 and 500 pg mL^{-1} of SPP1 and GAS6 proteins, respectively. Relative standard deviation (RSD) values of 6.8 and 8.0 % for SPP1 and GAS6, respectively, underlined the reliability of the manufacturing and detection processes. In addition, a similar study was performed using single SPCEs, calculating the RSD value for 10 immunosensors prepared in two scenarios: i) on the same day, and ii) on 10 different days. The results shown in Table 1 gave RSD values below 10 % in all cases, supporting the suitability of the procedures used.

Key factors in the implementation of methodologies for decentralized routine determinations using portable devices are the simplicity of the protocols involved and the shortening of the assay time. To achieve this, independent batches of CAb-functionalized and ET-blocked μMPs (ET/CAb-μMPs) were prepared on the same day and stored in filtered PBS at 4 °C. Since the storage stability of ET/CAb-μMPs for GAS6 was evaluated in a previous work [13], we tested the storage stability of the ET/CAb-μMPs used to prepare the immunoplatform for SPP1 using single SPCEs and measuring 0 and 500 pg mL^{-1} each control day. The results displayed in Fig. S2 (in the Supporting Information) show that the P/B ratios remained virtually unaffected for at least 30 days after the ET/CAb-μMPs preparation (longer times were not tested), thus confirming the feasibility to carry out the determination in only 60 min. Moreover, it is important to note that this assay time may be further reduced by decreasing both the incubation times of the bDAb/SPP1 mixture and the enzyme label from 30 to 15 min, without a significant loss of sensitivity.

3.4. Analysis of clinical samples

The single and dual immunoplatforms were applied to the analysis of both target proteins in aqueous humor from ICL as controls and patients diagnosed with CAT and GLAU. In addition, as a proof of concept, the determinations were carried out in tear samples from a healthy volunteer.

Prior to the analysis, the potential matrix effect was evaluated, by subjecting the samples to different dilutions (1/100 or 1/50). The slope values of the calibration plots constructed for each protein with the single SPCE immunoplatforms in buffer solution were compared with those calculated by constructing calibration graphs in 2 representative samples of each type of aqueous humor (ICL, CAT, and GLAU). According to the results obtained (see Table S3 in the Supporting Information), no apparent matrix effect was observed working with the

Table 2
Concentrations of SPP1 and GAS6 (in ng mL^{-1}) determined using the developed single immunoplatforms in different aqueous humor samples.

		SPP1 Immunoplatform		GAS6 Immunoplatform	
Sample	Code	[SPP1][a]	$RSD_{(n = 3)}$, %	[GAS6][a]	$RSD_{(n = 3)}$, %
ICL	**4**	85 ± 4	2.0	5.8 ± 0.2	1.8
	8	25.6 ± 0.8	1.2	9.2 ± 0.9	3.9
	24	52 ± 8	6.1	6.2 ± 0.6	3.8
	39	23 ± 2	3.1	5.1 ± 0.4	3.1
	41	29 ± 2	2.9	12.6 ± 0.8	2.7
CAT	**18**	33 ± 1	1.0	10.6 ± 0.6	2.4
	23	35 ± 1	1.6	10.3 ± 0.9	3.7
	66	62 ± 2	1.1	12.8 ± 0.8	2.4
	75	83 ± 17	8.4	11 ± 1	3.7
	80	69 ± 9	5.3	11.3 ± 0.8	2.9
GLAU	**3**	165 ± 18	4.3	16.1 ± 0.8	2.1
	11	108 ± 18	6.9	12.3 ± 0.8	2.5
	12	56 ± 4	2.7	19.2 ± 0.7	1.5
	28	181 ± 14	3.2	21 ± 2	3.1
	31	141 ± 8	2.4	21.2 ± 0.9	1.8

[a] Mean value ± $ts/\sqrt{n}$; n = 3; α = 0.05.

samples diluted 50 (GAS6) or 100 (SPP1) times.

Consequently, quantification of both proteins was performed by direct interpolation of the amperometric responses obtained for the diluted samples into the corresponding calibration graph prepared with standard solutions.

Since this was the first study using electroanalytical technologies for the analysis of aqueous humor samples, 15 samples (5 from each sample group) were analyzed using the single immunoplatforms. The results obtained are summarized in Table 2.

As expected, significant higher SPP1 and GAS6 concentrations were found for GLAU samples in comparison to ICL samples. In addition, larger concentrations of GAS6 were found in CAT samples versus ICL controls, whereas no significant differences were observed for SPP1 in CAT in comparison to controls.

After confirming the possibility of analyzing this type of matrix with the single immunoplatforms, 6 of these samples (2 from each of the 3 types of samples) were analyzed with the dual immunoplatform. The results, shown in Fig. 5 and summarized in Table 3, are fully consistent with those provided by the single immunoplatforms.

As expected, a high correlation between the results provided by the dual immunoplatform and the single ones was observed for SPP1 and GAS6, highlighting the usefulness of the dual technology for the simultaneous monitoring of both glaukers (Fig. S3 in the Supporting Information). Additionally, we compared these results with those reported using ELISA methodologies [2]. Importantly, the trends observed for SPP1 and GAS6 levels in aqueous humor samples from glaucoma and cataract patients versus controls were consistent across methodologies (ELISA and the electrochemical immunoplatform), with similar diagnostic ability of cataracts and glaucoma. However, although the concentrations determined using the electrochemical immunosensor were within the $ng{\cdot}mL^{-1}$, they were approximately 5-fold and 10-fold higher for SPP1 and GAS6, respectively, than those obtained by ELISA. These discrepancies can be attributed both to using different analytical methodologies, involving not only different modes of detection but also immobilization of the capture antibody through different strategies on different supports (adsorption on the ELISA plate and covalent immobilization using EDC/NHSS chemistry on HOOC-μMPs), and to the analysis of different clinical sample sets, whose target concentration can be different because of the interindividual variability.

Furthermore, an analysis of the results provided by the dual immunoplatform was performed by ROC curve analysis to evaluate the potential of discrimination between ICL controls, and CAT and GLAU patients (Fig. 6). The detailed analysis of the ROC curves showed a full discrimination (AUC, sensitivity, and specificity of 100 %) ability for GAS6 between ICL controls and CAT, and ICL controls and GLAU, whereas SPP1 showed 96 % AUC, 100 % sensitivity, and 80 % specificity

Table 3
SPP1 and GAS6 concentrations (in ng mL^{-1}) provided by the dual immunoplatforms in the aqueous humoral samples analyzed.

Sample	Code	[SPP1][a]	$RSD_{(n = 3)}$, %	[GAS6][a]	$RSD_{(n = 3)}$, %
ICL	8	25 ± 4	6.4	8 ± 2	11.2
ICL	39	27 ± 7	10.2	5.8 ± 0.2	1.7
CAT	18	29 ± 3	4.3	9 ± 1	6.1
CAT	23	32 ± 8	9.9	8 ± 1	5.4
GLAU	3	130 ± 27	8.3	15 ± 3	6.9
GLAU	31	156 ± 15	3.9	19 ± 5	10.2

[a]Mean value ± $ts/\sqrt{n}$; n = 3; α = 0.05.

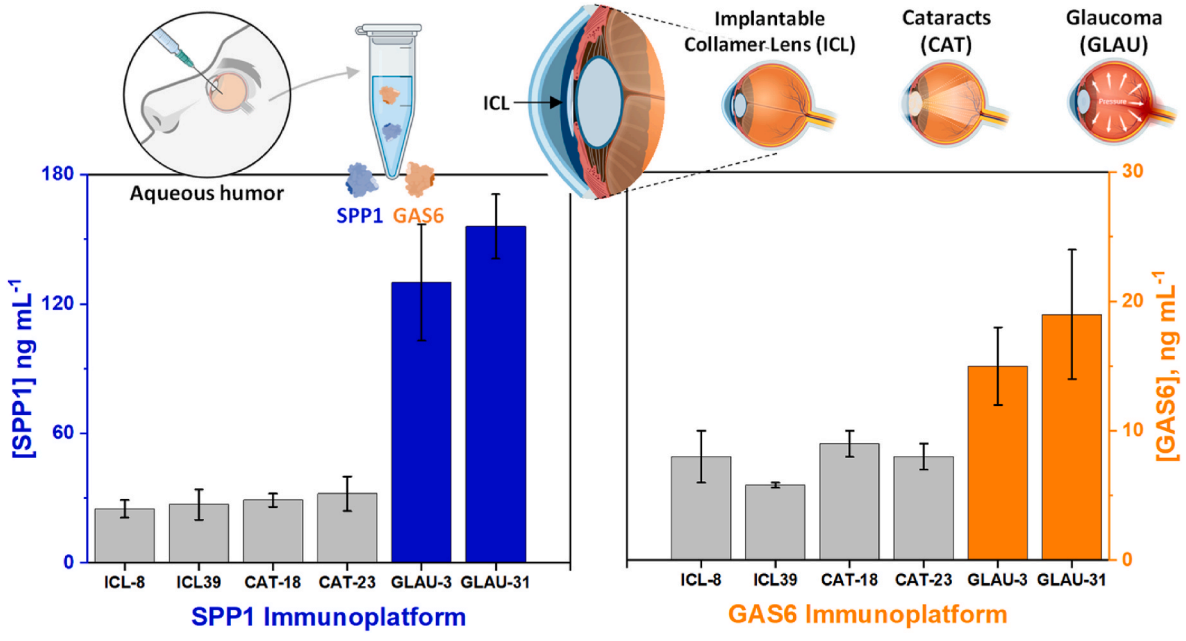

Fig. 5. SPP1 and GAS6 concentrations determined with the dual immunoplatforms in the aqueous humor samples analyzed. Created in part with biorender.com.

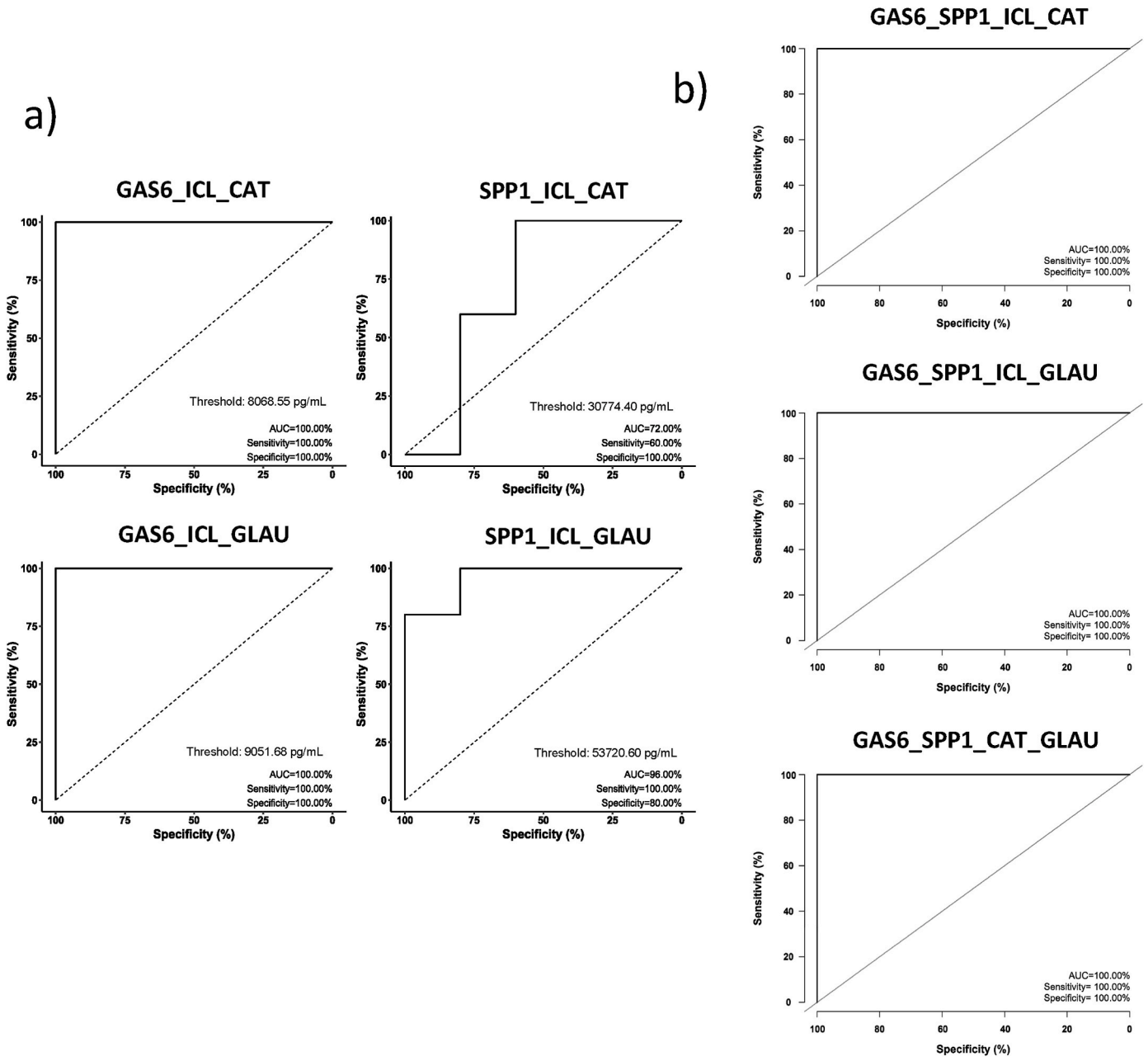

Fig. 6. Diagnostic potential of the determination of GAS6 and SPP1 in aqueous humor samples. The diagnostic potential for the determination of GAS6 and SPP1 was evaluated using ROC curves for the indicated comparisons, individually (a) or in combination (b). The cut-off value (threshold) for the indicated discrimination is shown in the inset of each individual ROC curve.

to discriminate ICL controls from GLAU patients, and 72 %, 60 %, and 100 % AUC, sensitivity, and specificity, respectively, for the discrimination between ICL and CAT. Additionally, the analysis of these quantitative results by the ROC curves allowed the establishment of the best cut-off values for the discrimination between ICL and CAT or GLAU with SPP1 and GAS6. Finally, by combining both markers, full discrimination between ICL controls and GLAU, between ICL and CAT, and even between CAT and GLAU patients, was achieved. These data showed the usefulness of the developed dual bioplatform for the discrimination between GLAU, CAT and ICL by evaluating the levels of GAS6 and SPP1. Collectively, these findings aligned with the emerging role of GAS6 and SPP1 as biomarkers associated with GLAU pathophysiology, where their altered levels correlate with disease progression and severity.

Finally, and as mentioned before, a proof-of-concept was made to check the potential of the dual technology for a less invasive diagnostic ability by performing the determination of the two target proteins directly in tear samples from a healthy volunteer. The results shown in Fig. 7 support the possibility of detecting the presence of these markers in this type of sample.

4. Conclusion

This study reports the first dual electrochemical immunoplatform for the simultaneous detection of SPP1 and GAS6 proteins in aqueous humor and tear samples. The optimized working conditions allowed the simple, rapid, sensitive, and selective determination of both biotargets, with LODs of pg mL^{-1}. Compared to conventional ELISA, the developed immunoplatform offers significant advantages, including reduced assay time, dual determination, and compatibility with point-of-care testing.

The clinical applicability of the immunoplatform was validated

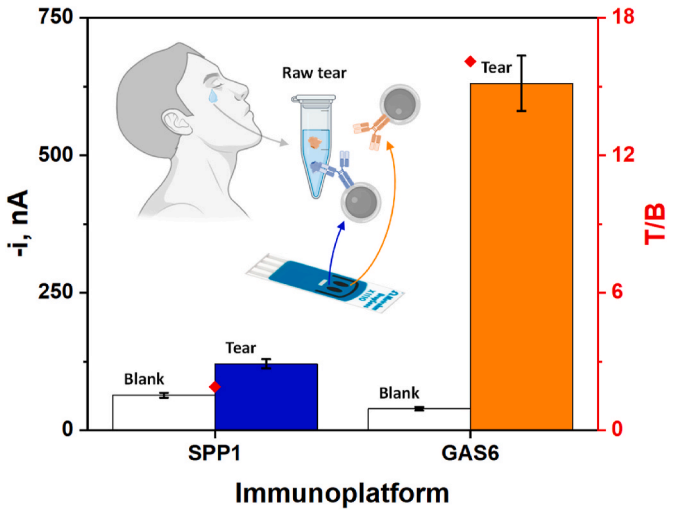

Fig. 7. Amperometric responses provided by the dual immunoplatform for the two target proteins directly in tear samples from a healthy volunteer. Created in part with biorender.com.

through the analysis of tear and aqueous humor samples from ICL, CAT, and GLAU patients. ROC curve analysis further confirmed the diagnostic usefulness of SPP1 and GAS6 to discriminate between ICL controls and GLAU, ICL and CAT, as well as CAT patients from GLAU patients, with the highest sensitivity and specificity (100 %).

In summary, this dual electroanalytical technology not only pioneeringly demonstrates the applicability of electroanalytical methods to the analysis of these ocular liquid biopsies but also highlights the potential of the two analyzed targets as "glaucoma drivers", thus representing a significant advance in the diagnosis of glaucoma, providing a reliable, rapid and minimally invasive approach for its early detection and monitoring of its progression.

CRediT authorship contribution statement

Eloy Povedano: Writing – review & editing, Writing – original draft, Methodology, Investigation. **Raquel Rejas-González:** Writing – review & editing, Writing – original draft, Methodology, Investigation. **Ana Montero-Calle:** Writing – review & editing, Writing – original draft, Methodology, Investigation. **Beatriz Arévalo:** Writing – review & editing, Investigation. **Alejandro Valverde:** Writing – review & editing, Investigation. **Natalia Pastora Salvador:** Writing – review & editing, Resources, Investigation. **María José Crespo Carballés:** Writing – review & editing, Resources, Investigation. **Juan Sánchez-Naves:** Writing – review & editing, Resources, Investigation. **José M. Pingarrón:** Writing – review & editing. **Rodrigo Barderas:** Writing – review & editing, Writing – original draft, Resources, Funding acquisition, Conceptualization. **Susana Campuzano:** Writing – review & editing, Writing – original draft, Supervision, Resources, Funding acquisition, Conceptualization. **Ana Guzman-Aranguez:** Writing – review & editing, Writing – original draft, Resources, Funding acquisition, Conceptualization.

Declaration of competing interest

The authors declare that they have no known competing financial interests or personal relationships that could have appeared to influence the work reported in this paper.

Acknowledgements

The financial support from PI23/00607 grant from the AES-ISCIII program, co-financed with FEDER funds to A.G-A., the financial support of PID2022-136351OB-I00 grant funded by MCIN/AEI/10.13039/501100011033 and by "ERDF A way of making Europe" to S.C., and the financial support from PI20CIII/00019 and PI23CIII/00027 grants from the AES-ISCIII program cofounded by FEDER funds to R.B. are greatly acknowledge. R.R.-G. acknowledges the PFIS predoctoral (C.22-A/45-PREDOC) contract supported by the AES-ISCIII program (AESIRRHH).

Appendix B. Supplementary data

Supplementary data to this article can be found online at https://doi.org/10.1016/j.talanta.2025.128438.

Data availability

All data generated or analyzed during this study are included in this published article and the supporting information file

References

[1] F. Li, D. Wang, Z. Yang, Y. Zhang, J. Jiang, X. Liu, K. Kong, F. Zhou, C.C. Tham, F. Medeiros, Y. Han, A. Grzybowski, L.M. Zangwill, D.S.C. Lam, X. Zhang, The AI revolution in glaucoma: bridging challenges with opportunities, Prog. Retin. Eye Res. 103 (2024) 101291, https://doi.org/10.1016/j.preteyeres.2024.101291.
[2] R. Rejas-Gonzalez, A. Montero-Calle, A. Valverde, N.P. Salvador, M.J.C. Carballes, E. Ausin-Gonzalez, J. Sanchez-Naves, S. Campuzano, R. Barderas, A. Guzman-Aranguez, Proteomics analyses of small extracellular vesicles of aqueous humor: identification and validation of GAS6 and SPP1 as glaucoma markers, Int. J. Mol. Sci. 25 (13) (2024), https://doi.org/10.3390/ijms25136995.
[3] I.V. Wagner, M.W. Stewart, S.K. Dorairaj, Updates on the diagnosis and management of glaucoma, Mayo Clin Proc Innov Qual Outcomes 6 (6) (2022) 618–635, https://doi.org/10.1016/j.mayocpiqo.2022.09.007.
[4] H. Jayaram, M. Kolko, D.S. Friedman, G. Gazzard, Glaucoma: now and beyond, Lancet 402 (10414) (2023) 1788–1801, https://doi.org/10.1016/S0140-6736(23)01289-8.
[5] N.E.I. EEUU. https://www.nei.nih.gov/, 2025. (Accessed 9 April 2025).
[6] H. Jayaram, Intraocular pressure reduction in glaucoma: does every mmHg count? Taiwan J Ophthalmol 10 (4) (2020) 255–258, https://doi.org/10.4103/tjo.tjo_63_20.
[7] V.M. Beutgen, J. Graumann, Advances in aqueous humor proteomics for biomarker discovery and disease mechanisms exploration: a spotlight on primary open angle glaucoma, Front. Mol. Neurosci. 17 (2024) 1397461, https://doi.org/10.3389/fnmol.2024.1397461.
[8] J. Nattinen, U. Aapola, P. Nukareddy, H. Uusitalo, Clinical tear fluid Proteomics-A novel tool in glaucoma research, Int. J. Mol. Sci. 23 (15) (2022), https://doi.org/10.3390/ijms23158136.
[9] R. Rejas-Gonzalez, A. Montero-Calle, N. Pastora Salvador, M.J. Crespo Carballes, E. Ausin-Gonzalez, J. Sanchez-Naves, S. Pardo Calderon, R. Barderas, A. Guzman-Aranguez, Unraveling the nexus of oxidative stress, ocular diseases, and small extracellular vesicles to identify novel glaucoma biomarkers through in-depth proteomics, Redox Biol. 77 (2024) 103368, https://doi.org/10.1016/j.redox.2024.103368.
[10] U.R. Chowdhury, S.Y. Jea, D.J. Oh, D.J. Rhee, M.P. Fautsch, Expression profile of the matricellular protein osteopontin in primary open-angle glaucoma and the normal human eye, Investig. Ophthalmol. Vis. Sci. 52 (9) (2011) 6443–6451, https://doi.org/10.1167/iovs.11-7409.
[11] S. Li, T.C. Jakobs, Secreted phosphoprotein 1 slows neurodegeneration and rescues visual function in mouse models of aging and glaucoma, Cell Rep. 41 (13) (2022) 111880, https://doi.org/10.1016/j.celrep.2022.111880.
[12] B. Shafit-Zagardo, R.C. Gruber, J.C. DuBois, The role of TAM family receptors and ligands in the nervous system: from development to pathobiology, Pharmacol. Ther. 188 (2018) 97–117, https://doi.org/10.1016/j.pharmthera.2018.03.002.
[13] C.M. Muñoz-San Martín, V. Pérez-Ginés, R.M. Torrente-Rodríguez, M. Gamella, G. Solis-Fernández, A. Montero-Calle, M. Pedrero, V. Serafín, N. Martínez-Bosch, P. Navarro, P.G. de Frutos, M. Batlle, R. Barderas, J.M. Pingarrón, S. Campuzano, Electrochemical immunosensing of growth arrest-specific 6 in human plasma and tumor cell secretomes, Electrochem. Sci. Adv. 2 (4) (2022), https://doi.org/10.1002/elsa.202100096.
[14] A. Klebes, H.C. Ates, R.D. Verboket, G.A. Urban, F. von Stetten, C. Dincer, S. M. Fruh, Emerging multianalyte biosensors for the simultaneous detection of protein and nucleic acid biomarkers, Biosens. Bioelectron. 244 (2024) 115800, https://doi.org/10.1016/j.bios.2023.115800.
[15] M. Sharafeldin, J.F. Rusling, Multiplexed electrochemical assays for clinical applications, Curr. Opin. Electrochem. 39 (2023), https://doi.org/10.1016/j.coelec.2023.101256.
[16] X. Ma, Y. Ge, N. Xia, Overview of the design and application of dual-signal immunoassays, Molecules (Basel) 29 (19) (2024), https://doi.org/10.3390/molecules29194551.
[17] N. Xia, G. Liu, Y. Chen, T. Wu, L. Liu, S. Yang, Y. Li, Magnetically-assisted electrochemical immunoplatform for simultaneous detection of active and total prostate-specific antigen based on proteolytic reaction and sandwich affinity

analysis, Talanta 270 (2024) 125534, https://doi.org/10.1016/j.talanta.2023.125534.
[18] A. Ahmad, G. Rabbani, S. Hosawi, O.A. Baothman, H. Altayeb, M.S.N. Akhtar, V. Ahmad, M.V. Khan, Ultrasensitive and label-free electrochemical immunosensor using gold nanoparticles deposited on a carbon electrode for the quantification of osteopontin: a serum-based oncomarker, Int. J. Biol. Macromol. 289 (2025) 138640, https://doi.org/10.1016/j.ijbiomac.2024.138640.
[19] A. Sharma, S. Hong, R. Singh, J. Jang, Single-walled carbon nanotube based transparent immunosensor for detection of a prostate cancer biomarker osteopontin, Anal. Chim. Acta 869 (2015) 68–73, https://doi.org/10.1016/j.aca.2015.02.010.
[20] F. Conzuelo, M. Gamella, S. Campuzano, D.G. Pinacho, A.J. Reviejo, M.P. Marco, J. M. Pingarron, Disposable and integrated amperometric immunosensor for direct determination of sulfonamide antibiotics in milk, Biosens. Bioelectron. 36 (1) (2012) 81–88, https://doi.org/10.1016/j.bios.2012.03.044.
[21] B.E.F. de Avila, V. Escamilla-Gómez, S. Campuzano, M. Pedrero, J.P. Salvador, M. P. Marco, J.M. Pingarrón, Ultrasensitive amperometric magnetoimmunosensor for human C-reactive protein quantification in serum, Sensor. Actuator. B Chem. 188 (2013) 212–220, https://doi.org/10.1016/j.snb.2013.07.026.
[22] D. Sarika, P.S.S. Ashwin Kumar, S. Arshad, M.K. Sukumaran, Purification and evaluation of horseradish peroxidase activity, Int. J. Curr. Microbiol. Appl. Sci. 4 (7) (2015) 367–375.
[23] M. Saud Al-Bagmi, M. Shahnawaz Khan, M. Alhasan Ismael, A.M. Al-Senaidy, A. Ben Bacha, F. Mabood Husain, S.F. Alamery, An efficient methodology for the purification of date palm peroxidase: stability comparison with horseradish peroxidase (HRP), Saudi J. Biol. Sci. 26 (2) (2019) 301–307, https://doi.org/10.1016/j.sjbs.2018.04.002.
[24] V.E. Lledo, H.A. Alkozi, J. Sanchez-Naves, M.A. Fernandez-Torres, A. Guzman-Aranguez, Modulation of aqueous humor melatonin levels by yellow-filter and its protective effect on lens, J. Photochem. Photobiol., B 221 (2021) 112248, https://doi.org/10.1016/j.jphotobiol.2021.112248.
[25] E. Povedano, A. Miglione, A. Montero-Calle, S. Cinti, J.M. Pingarron, R. Barderas, S. Campuzano, Electrochemical immunosensing of the neo-antigen collagen type I α 1 to assist in the personalized management of advanced colorectal cancer, Electroanalysis 37 (2025) e12052, https://doi.org/10.1002/elan.12052.
[26] R&DSystems, Human Osteopontin (OPN) ELISA kit, Cat. No.: DY1433 (15 plates) DuoSet® ELISA development system. https://www.rndsystems.com/products/human-osteopontin-opn-duoset-elisa_dy1433.
[27] R&DSystems, human Gas6 ELISA kit. Cat. no.: DY885B (15 plates) DuoSet® ELISA development system. https://www.rndsystems.com/products/human-gas6-duoset-elisa_dy885b.